Journal of Biomedical Optics

SPIEDigitalLibrary.org/jbo

ExiFRET: flexible tool for understanding FRET in complex geometries

Evelyne Deplazes
Dylan Jayatilaka
Ben Corry

SPIE

ExiFRET: flexible tool for understanding FRET in complex geometries

Evelyne Deplazes, Dylan Jayatilaka, and Ben Corry
University of Western Australia, School of Biomedical, Biomolecular and Chemical Sciences, Perth, Australia

Abstract. Fluorescence resonance energy transfer (FRET) can be utilized to gain low-resolution structural information by reporting on the proximity of molecules or measuring inter- and intramolecular distances. This method exploits the fact that the probability of the energy transfer is related to the separation between the fluorescent molecules. This relationship is well described for a single pair of fluorophores but is complicated in systems containing more than two fluorophores. Here, we present a Monte Carlo calculation scheme that has been implemented through a user-friendly web-based program called ExiFRET that can be used to determine the FRET efficiency in a wide range of fluorophore arrangements. ExiFRET is useful to model FRET for individual fluorophores randomly distributed in two or three dimensions, fluorophores linked in pairs or arranged in regular geometries with or without predefined stoichiometries. ExiFRET can model both uniform distributions and fluorophores that are aggregated in clusters. We demonstrate how this tool can be employed to understand the effect of labeling efficiency on FRET efficiency, estimate relative contributions of inter- and intramolecular FRET, investigate the structure of multimeric proteins, stoichiometries, and oligomers, and to aid experiments studying the aggregation of lipids and proteins in membrane environments. We also present an extension that can be used to study instances in which fluorophores have constrained orientations. [DOI: 10.1117/1.JBO.17.1.011005]

Keywords: fluorescence; spectroscopy; microscopy; simulations.

Paper 11213SS received Apr. 29, 2011; revised manuscript received Jul. 27, 2011; accepted for publication Jul. 28, 2011; published online Feb. 7, 2012.

1 Introduction

Fluorescence resonance energy transfer (FRET) spectroscopy is an important tool for investigating the structure and function of biological systems. FRET is based on the spontaneous nonradiative energy transfer from an excited donor to a suitable acceptor. The likelihood of this energy transfer, known as the FRET efficiency, shows a 6th-power dependence on the separation of donor and acceptor.[1] FRET is useful for determining the proximity of molecules and measuring inter- and intramolecular distances in the range of 10 Å to 100 Å. Among many other applications, FRET has been used to investigate the structure and dynamics of biomolecules,[2–4] study the aggregation behavior of proteins and lipids in membrane environments,[5–8] and to characterize polymeric materials.[9,10]

Quantitative measurements of FRET often aim to relate FRET efficiency and donor-acceptor separation. This relationship is well defined for a single donor-acceptor pair. However, many current applications of FRET include multiple donors and acceptors, and as a result the original single-distance expression cannot be used. One way of addressing this issue is to develop an analytical expression that describes FRET for a specific arrangement of donors and acceptors unique to a system of interest. The aim of this approach is to derive a function that relates FRET efficiency to a quantity of interest such as the radius of a tetrameric array of fluorophores or the density of fluorophores within a membrane. Analytical methods have been used to detect and characterize microdomains in membranes,[11–13] monitor lipid and protein interactions,[14,15] and to investigate proteins that form oligomeric complexes.[16–19] One of the advantages of analytical expressions is that they uniquely describe the FRET efficiency for a specific fluorophore distribution. Yet, this advantage also becomes a limitation as these models often show poor transferability to other systems. Furthermore, analytical expressions are often complex even for relatively simple systems, and fitting the necessary parameters might be required to make them suitable for the analysis. Another shortcoming is that most analytical methods are not suitable for modeling nonuniform distributions of fluorophores.

Numerical methods, such as Monte Carlo simulations (MCS), lend themselves well to modeling even complex arrangements of fluorophores and thus provide an alternative to analytical expressions. A series of studies have demonstrated that numerical methods are useful for the analysis and interpretation of data from FRET experiments. Wolber et al.[20] and Towles et al.[13] used results from MCS to validate analytical expressions. Singh and Raicu[21] investigated FRET in homogeneous and heterogeneous distributions of fluorophores and employed MCS to compare different methods of analyzing FRET data. Berney and Danuser[22] compared different methods of measuring and quantifying FRET efficiency and used MCS to provide independent reference values. Frederix et al.[23] showed that MCS can aid with the interpretation of data from microscopy experiments by simulating FRET between fluorophores on actin filaments, including the effect of photobleaching. Numerical methods proved to be especially helpful when modeling the nonuniform distributions of lipids and proteins in membrane

Address all correspondence to: Ben Corry, Research School of Biology, The Australian National University, Canberra, ACT, 0200, Australia. Tel: +61 2 61252655; Fax: +61 2 61250313; E-mail:ben.corry@anu.edu.au.

0091-3286/2012/$25.00 © 2012 SPIE

environments. Frazier et al.[24] used MCS to interpret the results from FRET experiments and investigate phase separation of a lipid mixture. Zimet et al.[25] modeled FRET between donors bound to membrane proteins and acceptors bound to lipids to study the effect of crowding on the quantum yield of the donor. Snyder and Freire[26] developed a numerical method to describe donor quenching of fluorophores in membranes. Kiskowski and Kenworthy[27] used MCS to demonstrate that FRET can be used to detect and characterize microdomains in membranes by studying the effect of clustering on FRET efficiency.

In contrast to analytical expressions, numerical methods do not define FRET as a function of a specific property or unique fluorophore arrangement. Rather, they model FRET by generating a set of donor and acceptor coordinates that emulate the real distribution of fluorophores found in the experiment. FRET efficiency is then simply calculated as a function of the donor-acceptor separations of all possible pairs. If implemented using a modular approach, numerical methods are flexible and can be used to investigate FRET in systems with different geometries or fluorophore distributions without the need to re-develop the method.

In a previous article,[28] we presented a simple and flexible Monte Carlo calculation scheme that was implemented using a FORTRAN program called ExiFRET. This program can be used to model FRET for a given distribution of fluorophores represented by coordinates that define their location in space. The system consists of individual fluorophores that are randomly distributed in two or three dimensions, or fluorophores that are arranged in regular geometries, such as when linked in pairs or pentamers. In this article, we present a user-friendly web-based version of this program that includes many extensions from the previous program. The aim of these extensions was to increase the flexibility of the program, thereby enabling it to generate fluorophore coordinates to emulate a large range of experiments. Furthermore, it also allows us to propose experiments that might be useful for obtaining structural information from complex systems.

In addition to the existing functionality, the extensions of the program include options to:

- generate fluorophore coordinates that can simulate hosts that contain only donors or acceptors. This is useful for modeling experiments where the fluorophores are attached to separate molecules. For example, for monitoring the self-association of proteins and lipids or reporting on the proximity of a ligand and its target protein.
- enforce a fixed stoichiometry of donors and acceptors within each host. This is useful for modeling heteromeric proteins with a known stoichiometry of subunits.
- model a reduced labeling efficiency in order to quantify its effect on FRET efficiency.
- model FRET for fluorophores that are arranged in clusters (i.e., aggregated into circular micro-domains). This has the potential to aid in the analysis of FRET experiments aimed at monitoring the aggregation behavior of lipids and proteins in membrane environments.
- calculate FRET for a set of user-provided fluorophore coordinates. This allows the program to be used to model FRET for any configuration of fluorophores.
- to model FRET between fluorophores with constrained orientations by accounting for the fluorophore's position in space, orientation, and mobility of the transition dipoles.

ExiFRET is available as a web-based version that allows the online execution of the program. The output can be retrieved from the website as simple text files. The website (www.exifret.com) also contains documentation of all input parameters and example input files for the data presented in this paper.

The remainder of the article is organized as follows: The Methods section provides a short summary of the Monte Carlo simulation scheme and describes how the new options were implemented into the existing program. The Results section outlines some examples of how these new input parameters can be used to investigate a range of different FRET experiments.

2 Methods

The Monte Carlo simulation scheme presented in this paper is an extension of the previously described ExiFRET .[28] The following section only provides a short overview of the steps required to generate the coordinates of fluorophores and calculate the FRET efficiency and lists the underlying theoretical assumptions. For a more detailed description of the individual steps and the theoretical background, the reader is referred to the previous publication.[28]

2.1 *Monte Carlo Simulation Scheme*

The aim of the simulation scheme is to calculate the FRET efficiency for different arrangements of fluorophores in two or three dimensions. The simulation system is defined by a set of parameters that are provided by the user as an input file. Table 1 gives a short description of the main input parameters. The process of FRET is simulated by modeling the incoming radiation as a series of discrete photons that are "played" according to a predefined time schedule. The incoming photons that are absorbed cause excitation of an available donor. Relaxation of the donor can occur via fluorescence or by transfer of energy to an available acceptor. The time for the relaxation is chosen based on the rate constant of these processes. By keeping a count of the number of fluorescence and energy transfer events, the overall FRET efficiency is calculated.

Figure 1 illustrates a schematic overview of the steps involved in calculating the FRET efficiency. In Step 1, a set of fluorophore coordinates in two or three dimensions is created based upon the input parameters. The coordinates are generated by an annealing procedure that prevents the fluorophores from overlapping. The simulation allows for regular geometries of particles by assigning fluorophores into so called n-mers, which consist of n fluorophores linked in a fixed relative orientation. For $n = 1$, the individual fluorophores are distributed randomly; while for $n = 2$, the fluorophores are linked as pairs. For $n \geq 3$, the fluorophores are regularly distributed either on a circle or sphere (3-D only) of a specified radius or hexagonally packed into tight oligomers (2-D). In Step 2, the fluorophores are randomly assigned a type (donor or acceptor) while enforcing the donor-acceptor ratio (P_{donor}) and stoichiometries ($da_{stoichiometry}$, $da_{separate}$), as defined in the input file. The transfer probability of each possible donor-acceptor pair based on the fluorophore separation and the provided R_0 value is calculated in Step 3. An excitation schedule is prepared to simulate the flux

Table 1 Values and meanings of input parameters for the ExiFRET program. Examples of input files can be found on the ExiFRET website (www.exifret.com).

Parameter	Allowed values	Meaning
User coordinates	True or false	True: fluorophore coordinates are provided by the user as an input file. False: fluorophore coordinates are generated by the program.
System dimension	2 or 3	Fluorophores are arranged in either 2-D or 3-D
Hexagonal oligomers	True or false	Used to simulate a system with single hexagonally packed *n*-mers. True: generates hexagonally packed oligomers. False: creates *n*-mers where the fluorophores are distributed on a circle (2-D) or sphere (3-D).
n-mer size	≥1	For $n = 1$, individual fluorophores are distributed randomly. For $n = 2$, fluorophores are linked in pairs with a specific separation. For $n \geq 3$, fluorophores are distributed on the radius of a circle (2-D or 3-D systems) or a sphere (3-D systems only).
Radius	≥0	Defines the size of the *n*-mer. The radius can be thought of as that of the host protein to which the probes are attached.
Density	>0	Density at which the *n*-mers are distributed through the system, in *n*-mers per $Å^2$ (2-D) or *n*-mers per $Å^3$ (3-D).
da stoichiometry	True or false	True: *a* fixed stoichiometry of donors and acceptors within each *n*-mer is enforced, as defined by the number of acceptors per *n*-mer and donors per *n*-mer. False: produces *n*-mers of mixed stoichiometries.
da separate	True or false	True: each *n*-mer contains only donors or only acceptors. False: fluorophores are randomly assigned as donors or acceptors and, hence, produces *n*-mers that contain both donors and acceptors
Second radius	True or false	True: two different radii are used to avoid overlapping the hosts and to determine the separation of the fluorophores for calculating FRET efficiency.
Avoid overlap	True or false	True: the fluorophores are arranged such that no *n*-mers overlap by using an excluded volume around each *n*-mer. False: no excluded volume is used and *n*-mers can overlap.
Planar *n*-mers	True or false	Active only if the system's dimension is 3. True: *n*-mers are distributed in a plane (i.e., a cricle). False: distributed in a sphere.
Clusters	True or false	True: *n*-mers are arranged in clusters. The system is defined by the cluster size and the number of clusters. False: n-mers are arranged in a random and homogeneous distribution.
R_0	≥1	Characteristic distance of the donor-acceptor pair, in Å
Configurations	≥1	Number of configurations used for calculating the average FRET efficiency of a given system.
Donor probability (P_{donor})	$0 < P_{donor} < 1$	Probability of any fluorophore being a donor (related to the d:a ratio).
Labeling efficiency (l)	$0 < l \leq 1$	Defines the proportion of sites that are labeled as a donor or acceptor.
Particles	≥1	Number of n-mers.
Photons	≥1	Number of absorbed photons used per configuration.
Irradiance	>0	Irradiance of the illuminating laser, in $W/\mu m^2$.
Wavelength	>0	Wavelength of the illuminating laser, in nm.
Extinction coefficient	>0	Extinction coefficient of donor, in $cm^{-1}M^{-1}$.
Donor lifetime	>0	Fluorescence lifetime of the donor in the absence of the acceptor, in ns.
Acceptor lifetime	>0	Fluorescence lifetime of acceptor, in ns.

of photons generated by the laser (Step 4). The rate at which the photons strike the system depends on the light intensity, which is modeled by calculating the flux of the photons based on the irradiance and the wavelength of the laser. The number of photons that are absorbed by the fluorophores depends on the number of donors in the system and the extinction coefficient. While previous calculations[28] suggest that typical laser irradiance values do not significantly influence FRET

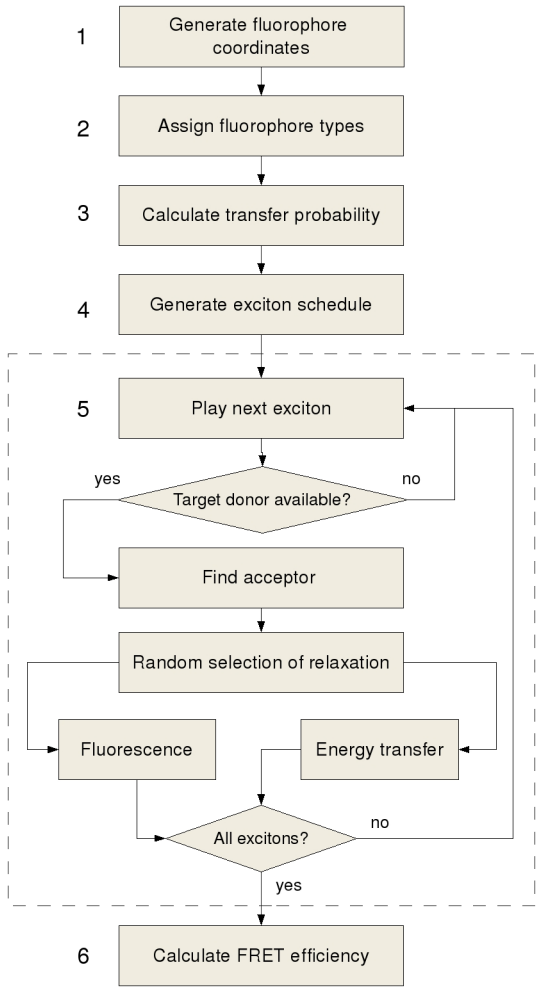

Fig. 1 Schematic representation of the steps involved in the Monte Carlo simulation scheme for calculating the FRET efficiency of any arrangement of fluorophores.

efficiencies, caution should be applied when using bright lasers or long lifetime acceptors. In Step 5, the energy transfer is modeled by playing the photons based on a predefined schedule. For each photon, the algorithm randomly chooses a donor from a previously generated list. This list excludes donors that have been previously excited and have not relaxed. The donor releases its energy either via fluorescence or energy transfer to an acceptor based on the relative probability of each process. The process of playing photons is repeated for the entire excitation schedule. A total count of the fluorescence and FRET events is maintained and subsequently used to calculate the FRET efficiency for that specific configuration of fluorophores (Step 6). The entire procedure, steps 1 through 6, is repeated for a large number of configurations (we typically use >1000) in order to calculate an average FRET efficiency for a given set of input parameters.

All of the extensions described in Sec. 2.3, apart from the case of constrained orientations, are concerned with the arrangement of the fluorophores. Hence, the extensions described only involved changes to the modules that generate the fluorophore coordinates and assign fluorophore types (Step 1 and 2). The overall scheme for modeling the incoming photons and calculating the FRET efficiency for a given configuration remains unchanged. Examples of input files can be found on the ExiFRET website (www.exifret.com).

2.2 *Assumptions*

The calculations in ExiFRET are based on a series of assumptions that might affect the validity and applicability of the predicted FRET efficiency:

- The algorithm does not model transfer between 2 donors or 2 acceptors (homo-FRET) or multiple transfer events for single packets of energy.
- Every photon absorbed by a donor has one of two fates: it is released via fluorescence or transfers energy to an available acceptor. Although in reality the excited state of the donor can decay by other mechanisms, these are not modeled in ExiFRET. This assumption does not affect the results of our calculations because the FRET efficiency is calculated from the ratio of the number of photons released via fluorescence and the number of photons that undergo energy transfers, and this will remain unchanged if some photons are lost from the donor by other decay mechanisms. Similarly, the mechanism of de-excitation of the acceptor does not affect the mode of relaxation of the donor and, hence, does not change the ratio of FRET and fluorescence events.
- The calculations assume that when multiple FRET acceptors are present, the quantum of energy is either released from the donor or transferred *in toto* to only one of the acceptors present. Furthermore, the transfer pathway of each donor is independent and, thus, the overall transfer rate for a given donor is the sum of the individual transfer pathways (referred to as the "kinetic model"[29]). The overall FRET efficiency is summed over all donors. These assumptions have been well validated for cases of multiple fluorophores, particularly through the measurement of FRET in solution,[28,30] or cases with a single donor and multiple acceptors,[31] although a recent study questions its validity in specific situations.[29]
- The value of R_0 depends on, among other things, the relative orientation of the donor and acceptor transition dipoles, as given by the orientation factor κ^2. The algorithm in ExiFRET does not assume any particular value for κ^2 but instead leaves this to be specified by the user through the value of R_0 in the input file.
- The annealing procedure that assigns the fluorophore coordinates assures that no n-mers overlap by using an excluded volume around each n-mer where no other fluorophore can reside. This option can be disabled if desired.
- After the donor becomes excited at time T_e, it remains excited for a period T_d. The donor is unavailable until time $T_e + T_d$. T_d depends on the rate of energy release from the donor, which is given by the lifetime of the unquenched donor, the number of available acceptors, and the transfer probabilities of all donor-acceptor pairs.
- Similarly, if an acceptor becomes excited it remains excited for a period T_a, which depends on the acceptor lifetime. Although in reality the acceptor will only become excited at a time interval after the de-excitation

of the donor; here we assume the acceptor is unavailable in the time interval $T_e + T_a$.

2.3 *New Input Parameters*

2.3.1 *Clustering of fluorophores*

We have extended the annealing procedure to allow for the generation of coordinates for fluorophores arranged in circular clusters (for 2-D only). Figure 2 illustrates the difference between a random arrangement and fluorophores that have aggregated into clusters. These microdomains are modeled as a number of independent circular regions of high fluorophore concentration, as defined by the number of clusters and their size (defined by their radius). The annealing procedure randomly distributes the clusters within the system avoiding overlapping regions. Each fluorophore is randomly assigned to a cluster which creates regions of different local density while fulfilling the system-wide fluorophore density defined in the input file. The same annealing procedure is reused to randomly distribute the fluorophores within each cluster, thereby producing a final set of fluorophore coordinates that are used to calculate the FRET efficiency.

2.3.2 *Assignment of fluorophore type*

In the original simulation scheme, the fluorophores are randomly assigned to be donors or acceptors such that the system-wide donor-acceptor ratio matches the input parameter, P_{donor}. The new input, $da_{separate}$, allows the user to generate n-mers that contain only donors or acceptors (see Sec. 3.1 and Fig. 4). A new parameter, $da_{stoichiometry}$, allows the user to control the stoichiometry of the donors and acceptors within each n-mer. Although this procedure enforces a fixed ratio of donors and acceptors, their exact position within each n-mer is still randomly chosen.

2.3.3 *Size of the n-mer*

Fluorophores that are arranged in a regular geometry are very useful for modeling FRET in multimeric proteins where the fluorophores are attached to the individual subunits. In the calculation scheme, the size of the n-mers is defined by the radius of the circle or sphere on which the fluorophores are distributed in a fixed relative orientation. This radius is used in two steps of the algorithm. First, it is used in the annealing procedure to avoid overlapping the host molecules. Second, the radius is used to position the fluorophores themselves around the host. In fact, two different radii can now be defined for these two tasks: 1. the radius describing the size of the host molecule to avoid overlapping n-mers; 2. the radius that defines the n-mer formed by the fluorophores which defines the fluorophore positions (see Fig. 8, inset). To use two different radii, a logical input parameter (second radius) is set to true; otherwise only the larger radius is used.

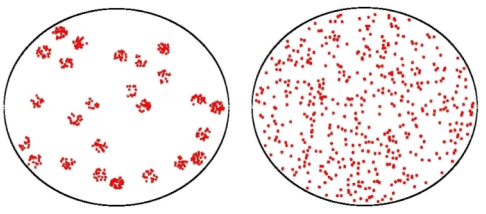

Fig. 2 ExiFRET can be used to model FRET for fluorophores in a uniform distribution (b) or aggregated into clusters (a).

2.3.4 *Labeling efficiency*

Reduced labeling efficiency can significantly lower the observed FRET efficiency. A new input parameter allows the user to specify a labeling efficiency to model the effect of unlabeled sites on the final FRET efficiency. Rather than simply scaling the final result of the calculation by the labeling efficiency, the input parameter is used when assigning fluorophore types. In addition to donors and acceptors, a new particle type, known as "empty," was created. The assignment of these empty sites is random such that each fluorophore in the system has an equal probability of being an unlabeled site. The labeling efficiency (le) effectively reduces the total number of fluorophores such that $n_{empty} = n_{total} - (1 * le)$, $n_{acceptor} = n_{total} * le * (1 - P_{donor})$ and $n_{donor} = n_{total} * le * P_{donor}$

2.3.5 *User-provided coordinates*

The extended version of ExiFRET allows the user to provide a text file with the positions and types of a set of fluorophore coordinates to describe any system they desire. In this case, Step 1 and 2 in the algorithm (Fig. 1) are bypassed and the x, y, and z coordinates, as well as the fluorophore type, are read from the text file. Other calculation parameters, such as the donor-acceptor ratio and the fluorophore density, are calculated from the input data. The calculation scheme then proceeds normally with Steps 3 through 5. The only difference is that in this case the FRET efficiency is calculated for the single configuration that is provided by the user and, hence, the final result is not averaged over many configurations.

3 Results

3.1 *Background Concentration*

One use of FRET is to determine the distance between two specific sites in a molecule based on measuring the FRET efficiency between a donor and acceptor that are attached to the same host (intramolecular FRET). Any occurrence of FRET between host molecules (intermolecular FRET) can interfere with these intramolecular events. The likelihood of intermolecular FRET increases with increasing host density, such as in samples with a high concentration of host molecules, or through an increase in the local concentration caused by the crowding of host molecules. This increase in intermolecular FRET will cause a systematic error and disrupt any effort to use the FRET efficiency of the donor-acceptor pair of the same host. It is usually impossible to experimentally determine the relative contributions of inter- and intramolecular FRET to the total observed FRET efficiency, hence the presence of intermolecular FRET introduces uncertainty. ExiFRET can be used to prepare a plot of FRET efficiency versus fluorophore separation (for a given density of fluorophores) that includes FRET from both inter- and intramolecular FRET and allows for the correct determination of intramolecular distances. Figure 3(a) shows the relationship between the FRET efficiency and the

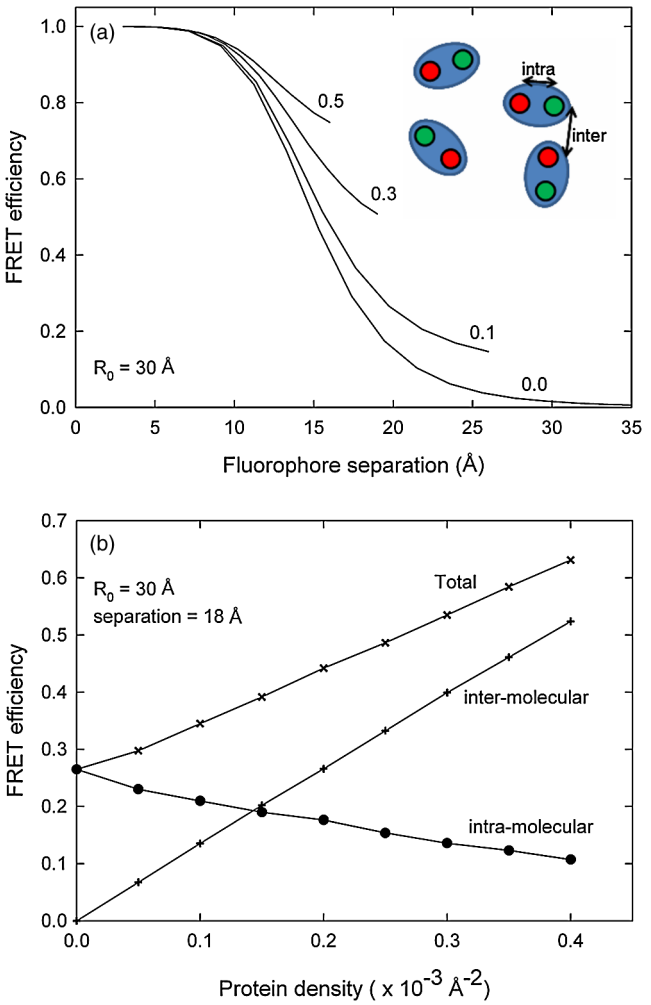

Fig. 3 (a) FRET efficiency versus fluorophore separation for hosts distributed in a 2-D environment containing a single donor-acceptor pair for a series of different n-mer surface densities (noted next to each curve in units of $\times 10^{-3}$ Å^2). (b) ExiFRET can be used to quantify the contribution of inter- and intramolecular FRET to the total FRET efficiency, as shown for host proteins (n-mers) distributed in a environment containing a single donor-acceptor pair. The total FRET efficiency increases with increasing surface density due to the increasing likelihood of intermolecular FRET. The values of the key parameters are shown in the figure. A complete and representative input file for this and the subsequent figures is given on the website (www.exifret.com).

donor-acceptor separation of a single host for different average densities of host molecules distributed in 2-D. The FRET efficiency is very different at different host concentrations, even with a fixed donor-acceptor separation for each host.

It is also possible to use ExiFRET to quantify the contributions of inter- and intramolecular FRET to the total observed FRET efficiency as a function of surface density. In Fig. 3(b), this is plotted for hosts containing a single donor-acceptor pair.

Alternatively, an estimate of inter- and intramolecular FRET can also be obtained by comparing plots of FRET efficiency versus surface density of systems with different combinations of mixed and separate donor-acceptor hosts [Fig. 4(a)]. The new input parameters, $da_{separate}$ and $da_{stoichiometry}$, were used to define three cases of similarly arranged fluorophores that show different combinations of inter- and intramolecular FRET. In case 1, the stoichiometry of the donors and acceptors within each n-mer is not fixed and both mixed and separate hosts are present ($da_{stoichiometry}$ = false, $da_{separate}$ = false). Therefore, both inter- and intramolecular FRET are possible. In case 2, each n-mer consists of a donor-acceptor pair by enforcing a fixed stoichiometry ($da_{stoichiometry}$ = true, $da_{separate}$ = false). This increases the likelihood of intramolecular FRET, resulting in an increase in the overall FRET efficiency. Case 3 describes n-mers that contain either only donors or only acceptors and, hence, removes the possibility of intramolecular FRET ($da_{stoichiometry}$ = false, $da_{separate}$ = true). This decreases the overall FRET efficiency. Provided the level of intermolecular FRET is equal in all cases, the contribution of intramolecular FRET in case 1 and 2 can be determined by subtracting the FRET efficiency of case 1 from the FRET efficiency of case 2 or 3. We confirmed this by calculating the relative contributions from inter- and intramolecular FRET for each case [Fig. 4(b)] and found that all three cases show very similar levels of intermolecular FRET efficiency. Therefore, this approach has the potential to be useful for estimating the relative contributions of inter- and intramolecular FRET over a range of fluorophore concentrations. Another interesting outcome of the simulation of these three cases is that intramolecular FRET decreases with increasing surface density. This means the contribution of intramolecular FRET to the total FRET efficiency decreases because the intermolecular FRET starts to compete with the intramolecular FRET.

3.2 *Multimeric Proteins and Oligomers*

Another possible use of FRET is to examine the physical dimensions of oligomeric proteins. Previous studies have used analytic expressions or numerical methods to determine the relationship between FRET efficiency and either the radius of the oligomer[28,32,33] or the number of subunits involved. Adair and Engelman[34] showed that FRET can be used to differentiate between dimers and larger oligomers. More recent studies have demonstrated that it is possible to quantify the number of subunits in larger oligomeric proteins and to estimate the fraction of proteins that remain present as monomers.[16–19,35] An advantage of using numerical methods, as described here, is that they can they account for intermolecular FRET (see Sec. 3.1) and can model clusters of oligomers (see Sec. 3.3).

In Fig. 5 we show how FRET efficiency depends on the physical size of the oligomers for oligomers containing between two and eight subunits with a fluorophore on each monomer that has been randomly assigned to be a donor or acceptor. This plot highlights the fact that none of these lines follow the $1/R^6$ relationship one would expect for donor-acceptor pairs. Having such a plot is crucial when using FRET to quantitatively investigate the structural changes that take place in multimeric proteins such as ion channels.[32,33]

ExiFRET also shows how the number of subunits in an oligomer can be determined from appropriate FRET experiments. Figure 6 shows plots of FRET efficiency versus donor probability (i.e., donor to acceptor ratio) for a series of ring-shaped oligomers with increasing numbers of subunits. Although all graphs are of similar shape, the maximum FRET efficiency shows a systematic shift to the left with an increasing number of subunits.

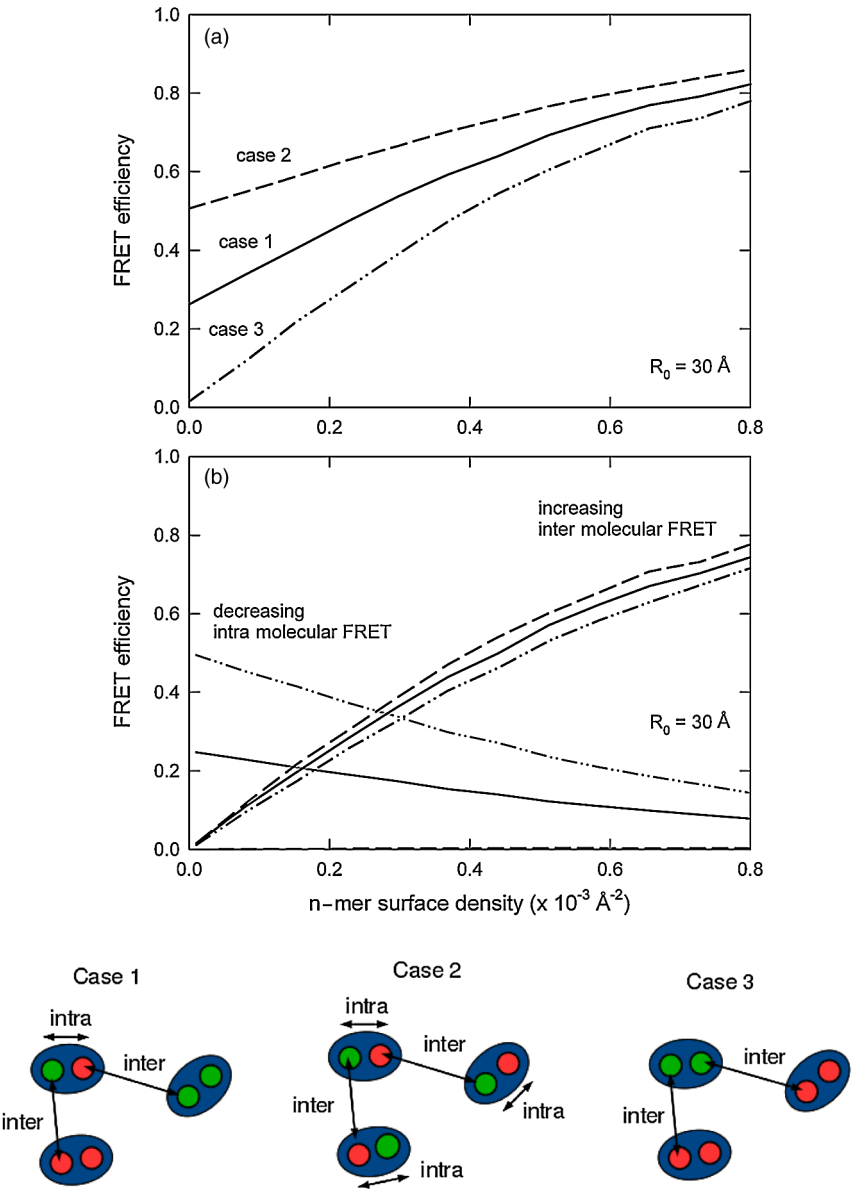

Fig. 4 FRET efficiency versus fluorophore density for three different labeling protocols of hosts with two fluorophores distributed in 2-D. Comparisons of the FRET efficiencies of the three cases can be used to quantify the contributions of inter- and intramolecular FRET. (a) The total FRET efficiency for each case. (b) Inter- and intramolecular FRET for each case. Note that the intramolecular FRET is always 0 for case 3. Case 1: every site has equal probability of being a donor or acceptor (solid lines). Case 1 is modeled using $da_{stoichiometry} = false$, $da_{separate} = false$. Case 2: each host has one donor and one acceptor (dashed lines). Case 2 is modeled using $da_{stoichiometry} = true$, $da_{separate} = false$. Case 3: each host has either two donors or two acceptors (dot-dot-dashed lines). Case 2 is modeled using $da_{stoichiometry} = false$, $da_{separate} = true$.

Plots of FRET efficiency versus multimer radius might also be used to investigate the effect of a fixed stoichiometry of different subunits in heteromeric proteins on FRET efficiency. Figure 7 shows plots of FRET efficiency versus multimeric radius for a series of pentamers with different stoichiometry of donors and acceptors in comparison with pentamers with random stoichiometry. Predicting the effect of stoichiometry of the subunits on the FRET efficiency might be useful for investigating multimeric proteins of unknown stoichiometry.

When using FRET to determine the radius of a multimeric protein, it might be necessary to consider the size of the fluorescent probe relative to the size of the host molecule. The observed FRET efficiency is based on the fluorophore positions, which are not necessarily equal to the positions of the host subunits to which the probes are attached. If the size of the fluorescent probe is small relative to the size of the host, this difference in positions might not be important. However, with large fluorescent probes or long linkers, significant differences can arise (see Fig. 8, inset). Figure 8 shows a plot of FRET efficiency versus fluorophore density that was calculated with and without considering the size of the fluorescent probe for pentamers of size 50 Å with probes with a linker length of 12 Å. The results show that deviations in the FRET efficiency can be as large as 10%.

3.3 *Labeling Efficiency*

The inability to label every targeted site on the host protein will lower the observed FRET efficiency, resulting in uncertainty if

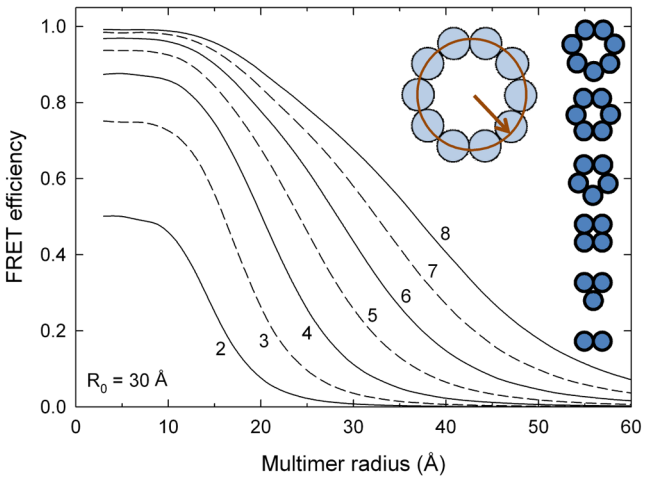

Fig. 5 FRET in multimeric proteins. The FRET efficiency is plotted versus the radius of the multimer in 2-D for a situation in which each subunit has equal probability of holding a donor or an acceptor. Numbers next to each curve refer to the number of subunits in the multimer (*n*-mer size). The different mulitmers are shown on the right.

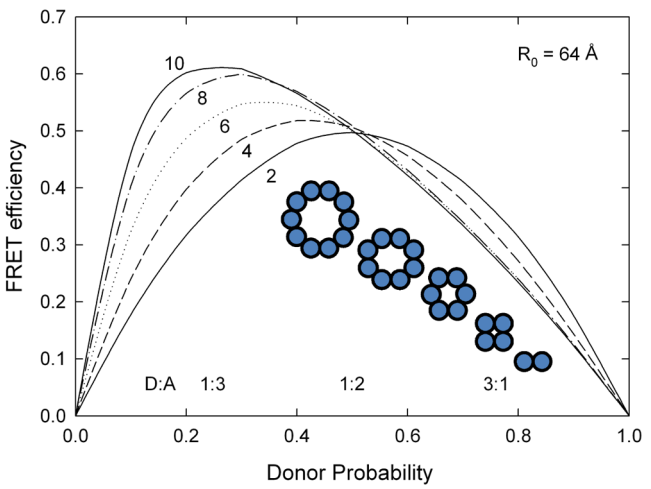

Fig. 6 FRET efficiency is plotted against donor probability for a series of oligomers of increasing *n*-mer size (given beside each curve) distributed in 2-D. The multimer radius in each case is chosen such that the FRET efficiency is 0.5 when the donor probability = 0.5.

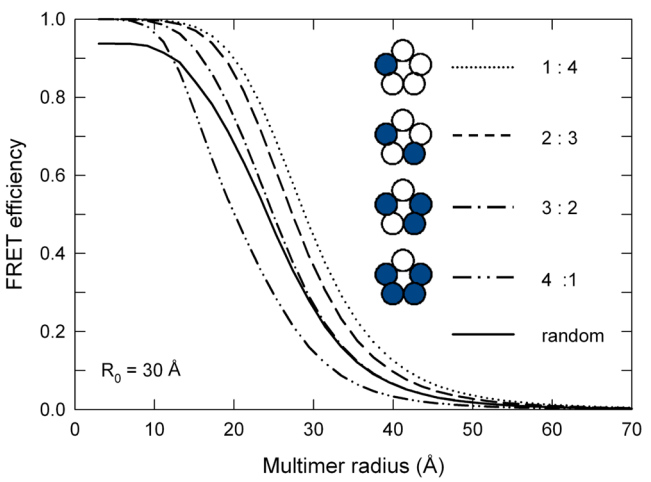

Fig. 7 FRET efficiency plotted against multimer radius for a set of pentameric proteins with different stoichiometries of donors and acceptors.

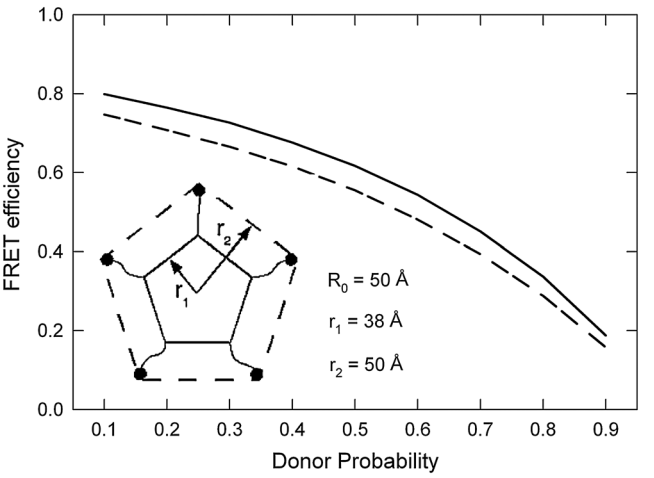

Fig. 8 Plot of FRET efficiency versus donor probability for fluorophores arranged in pentamers that are uniformly distributed in 2-D. Solid line: radius r_1 (38 Å) was used to avoid overlapping the pentamers and r_2 (50 Å) was used to generate fluorophore coordinates and calculate the FRET efficiency by considering the size of the fluorophores. Dashed line: a single radius (r_2) is used to generate the pentamer positions, fluorophore coordinates, and calculate the FRET efficiency.

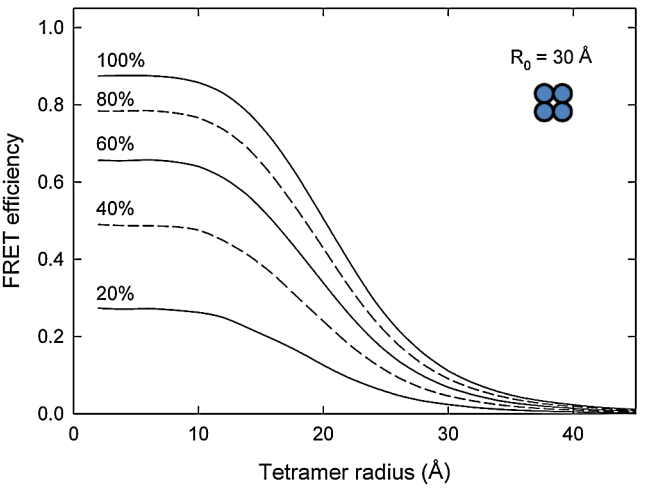

Fig. 9 Plots of FRET efficiency versus fluorophore separation for a series of tetramers distributed in 2-D with different labeling efficiencies, as shown beside each curve.

the data are used for quantitative analysis. ExiFRET can be used to quantify the effect of reduced labeling efficiency on FRET efficiency. In Fig. 9, we plot the FRET efficiency versus fluorophore separation in tetrameric arrangements of fluorophores for a series of labeling efficiencies. As expected, decreasing the percentage of sites that are labeled decreases the resulting FRET efficiency. If estimates of the likely labeling efficiency can be determined experimentally, such plots can be used to account for inefficient labeling or to obtain estimates of the uncertainty that is introduced into the FRET efficiency.

3.4 *Presence of Clusters or Microdomains*

The formation of microdomains in membrane environments has been associated with a range of physiological processes; hence, understanding the partitioning and aggregation of lipids and

proteins in membrane environments is important. The use of fluorescence anisotropy and FRET experiments for studying the spatial organization and co-localization of proteins in membranes was first demonstrated by Varma and Mayor[36] and Kenworthy.[37] A number of subsequent studies[7,8,38] have confirmed the use of FRET to indicate aggregation and detect microdomains (see Refs. 5 and 6 for reviews). This method exploits the fact that the aggregation of donors and acceptors in microdomains causes a local increase of fluorophore concentration, which results in an increase in the FRET efficiency when compared with systems with a random and homogeneous distribution of fluorophores.[7,25,39] However, as noted by Kiskowski and Kenworthy,[27] the presence of increased FRET is not enough evidence to demonstrate the existence of clusters; but the dependence of FRET on properties such as fluorophore density should be used to differentiate between microdomains and homogeneous random distributions of particles. For a clustered distribution, it can be expected that the FRET efficiency shows less dependence on the overall fluorophore concentration (i.e., surface density) as opposed to the linear relationship in a random and homogeneous distribution.[7,39] Zacharias et al.[40] used the same argument in FRET experiments to investigate the clustering of lipid-modified green fluorescent proteins. To demonstrate this, we used ExiFRET to prepare plots of FRET efficiency versus fluorophore surface density for random and clustered distributions. The results in Fig. 10(a) confirm that the lack of change in FRET with increasing surface density signals the presence of clusters.

Beyond simply detecting the presence of clusters, FRET can also be useful to extract information about the intradomain density of fluorophores and the size of the cluster. Figure 10(b) shows that the FRET efficiency depends on the fluorophore surface density inside the domain as well as on the physical size of the domain. Similar results were reported in a Monte Carlo study of FRET for disk-shaped domains.[27] They showed that intradomain FRET is fully described by the local acceptor density. Deducing the size of clusters from FRET efficiency is, however, a much harder task because there is often no unique solution. Different combinations of cluster size and intradomain density can result in the same FRET efficiency. Kiskowski and Kenworthy[27] found that simulations where donors and acceptors are co-localized inside microdomains cannot be used to extract the cluster size. Our own simulations of co-localized donor-acceptor clusters confirmed this, as we found that the FRET efficiency shows very small variations over a large range of cluster sizes (for a constant intradomain density). Yet, Kiskowski and Kenworthy showed that it is possible to determine the domain radius independently of the intradomain density by performing simulations where the donors and acceptors are not colocalized but where the donors are aggregated into domains surrounded by uniformly distributed acceptors.[27] Similarly, Towles et al.[13] presented a method that uses an analytical model in combination with Monte Carlo simulations to extract the domain size of nanoscale lipid rafts from time-resolved FRET data, although this method requires *a priori* knowledge of the phase diagram of the membrane system being investigated. Sharma et al.[38] used homo-FRET and theoretical analyse based on analytical expressions to study the size and surface organization of glycosylphosphatidylinositol (GPI)-anchored proteins in living cell membranes.

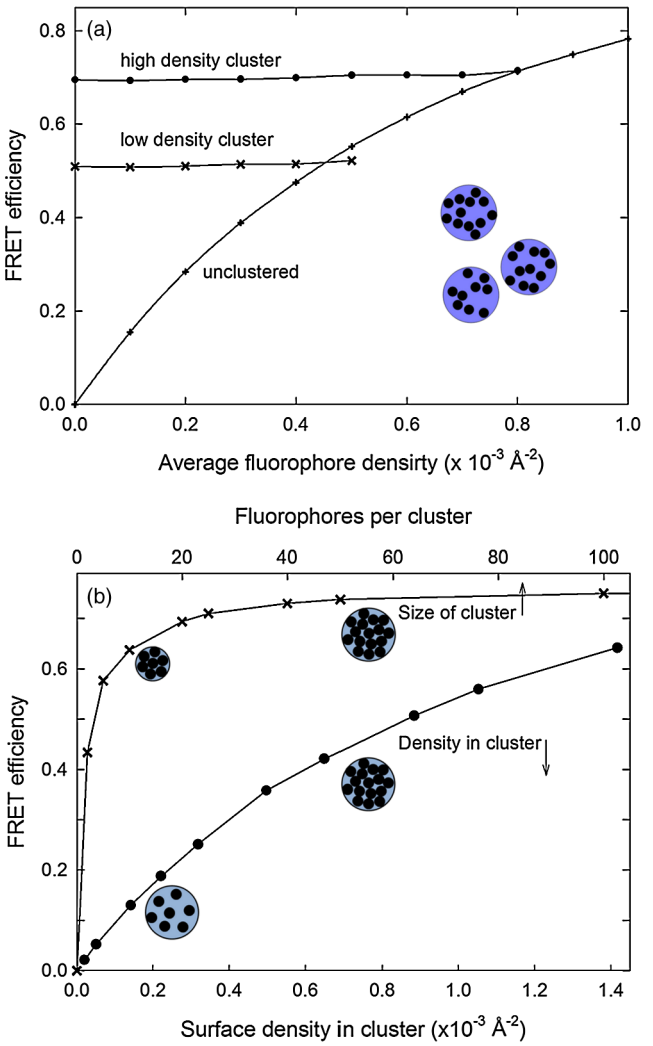

Fig. 10 (a) Plots of FRET efficiency versus fluorophore surface density for randomly arranged fluorophores (unclustered) and fluorophores arranged in low- and high-density clusters. The absence of changes in FRET efficiency can be used to detect clusters, while the magnitude of the FRET efficiency determines the local concentration in the cluster. (b) FRET efficiency is plotted versus fluorophore surface density when either the cluster dimension is the same but the internal density is varied (lower line), or the internal density is fixed but the size of the cluster changes (upper line).

The results in Figure 10 and the previously published findings[7,27] demonstrate that numerical methods, such as ExiFRET, can be very helpful for developing methods to use FRET for investigating microdomains and the aggregation behaviors of lipids and proteins. The flexibility of such methods means that clusters formed by individual fluorophores or multimeric proteins and oligomers can be studied without the need to adjust the method of calculating FRET.

3.5 *Fluorophores with Constrained Orientations*

All the examples discussed so far do not directly consider the relative orientation of the fluorophores. Rather, a system-wide value of R_0 is used for these calculations. In practice, the value of R_0 includes information about the relative fluorophore orientations through the so-called orientation factor κ^2. While the use of a system wide value of R_0 need not imply a specific value of

κ^2, it does not allow for the value of R_0 to depend on the specific direction in which the fluorophores are separated and how this compares to the orientations of the fluorophore transition dipoles.

To incorporate the fluorophore orientations directly into the Monte Carlo calculation scheme, we wrote a second program called thetaFRET. This has less functionality for the generation of fluorophore coordinates, but can be used to calculate the likely FRET efficiency of a set of fluorophores when information about both their positions and some information about their orientations are known. In this case, the fluorophore positions are uploaded from a coordinate file in a manner similar to the user-generated coordinates option of ExiFRET. In addition, the fluorophore orientations are modeled from random motion within a cone, which is described by the mean transition dipole orientation and the cone angle as additional columns in the coordinate file. FRET efficiencies can be calculated either in a dynamic orientational-averaging regime, in which the fluorophore motion is assumed to be faster than the energy transfer time (thus κ^2 is averaged over many possible fluorophore orientations), or in a static orientational-averaging regime, in which the FRET efficiency is calculated for each instantaneous set of fluorophore orientations.

As an example of this program, in Fig 11(a) we consider the FRET efficiency of a pair of fluorophores separated by a distance equivalent to R_0, as calculated assuming $\kappa^2 = 2/3$. Here, we plot FRET efficiency as a function of the orientational freedom of the fluorophores, as described by the size of the cone angle in which they can move. When the cone angle $\theta = 90$ deg, then the dyes have complete orientational freedom, and in the case of the dynamic averaging regime where $\kappa^2 = 2/3$ and, thus, the FRET efficiency equals 0.5. However, as the orientational freedom of the fluorophores is reduced, the FRET efficiency changes dramatically. κ^2 depends on the relative orientation of the mean transition dipoles. In this case, its value rises to 4 when the dipoles are aligned parallel to each other and the direction of their separation ($E \sim 0.86$) and to 1 when the dipoles are parallel to each other but perpendicular to the direction of separation ($E = 0.6$). Notably, FRET efficiencies are always lower in a static orientational-averaging regime than in an equivalent dynamic case.

To give an example of when this program may be useful, we indicate in Fig. 11(b) how it could be used to gain structural information. Here, we calculate the FRET efficiency as a function of the angle between the donor and acceptor transition dipoles (ϕ) assuming that they both lie in the plane perpendicular to the direction of their separation. This could be useful, for example, if we were attempting to determine the twist or bend of a DNA strand using fluorophores that were tightly embedded in the molecule (thus limiting the orientation of the molecule), as is the case with fluorophores that are nucleic base analogs.[41] If the fluorophores have no orientational freedom (i.e., $\theta = 0$), then the FRET efficiency varies from 0.6 when the fluorophores are parallel to 0.0 when they are perpendicular. As the fluorophores become more mobile (as the cone angle θ increases) the change in FRET with the rotational angle ϕ decreases. In the case of nucleic acid analogs, the cone angle is very small,[41] and, thus, a plot like this could be used to relate a measured FRET efficiency directly to the twist of the DNA strand.

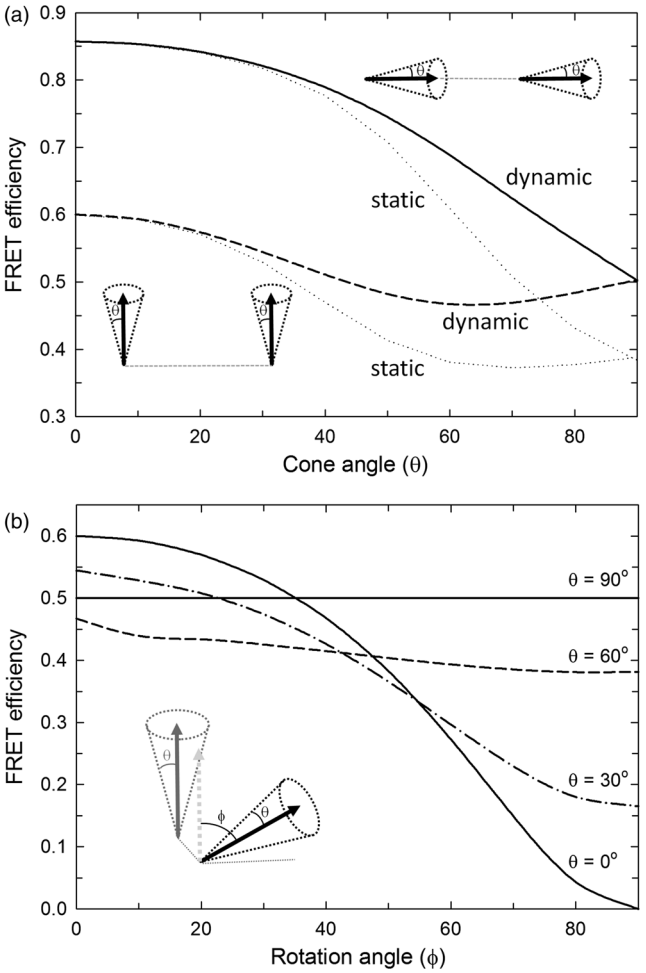

Fig. 11 FRET efficiencies for fluorophores with constrained orientations. (a) FRET efficiency is plotted for a pair of fluorophores versus their orientational freedom (measured by the cone angle θ). In all cases, the transition dipole orientations are in parallel, but in the upper lines they are also in parallel to the direction of fluorophore separation, while in the lower lines they are perpendicular to this direction. Solid and dashed lines show results that assume a dynamic orientational-averaging regime, while dotted lines show equivalent results that assume static averages. (b) The FRET efficiency is plotted as a function of the angle between the mean transition dipole orientation of the donor and acceptor (ϕ) where the dipoles are perpendicular to the direction of their separation. Results are shown assuming the transition dipole can move within a cone of angle 0, 30, 60, and 90-deg. In all cases the cone angle θ, of the donor and acceptor are equal.

4 Concluding Remarks

The examples presented in this paper and the referenced studies demonstrate the versatility and capability of FRET for obtaining structural information of biomolecules and for investigating the aggregation of proteins and lipids in membrane environments. However, this study also highlights the importance of considering the presence of more than one pair of fluorophores in the data analysis. The results showed that the relationship between the FRET efficiency and fluorophore separation can strongly deviate from the commonly used $1/R^6$ relationship for fluorophores arranged in regular geometries such as those found in multimeric proteins or oligomers. We developed a Monte Carlo simulation scheme and implemented it in a flexible and user-friendly program called ExiFRET that allows the user to

model FRET for individual fluorophores that are randomly distributed in two or three dimensions and fluorophores linked in pairs or arranged in regular geometries. We demonstrated how ExiFRET can be used to estimate the uncertainty in the FRET efficiency caused by reduced labeling efficiency, model FRET in multimeric proteins and oligomers, and investigate fluorophores arranged in microdomains. The effect of a constrained orientation of the fluorophores on FRET efficiency was demonstrated using a second tool called thetaFRET. More generally, this study demonstrates how numerical methods are very well suited to aid in the design and data analysis of FRET experiments.

Acknowledgments

This work was supported by funding from the Australian Research Council. E. Deplazes thanks the University of Western Australia for the Jean Rogerson Postgraduate scholarship.

References

1. T. Forster, "Zwischenmolekulare Energiewanderung und Fluoreszenz," *Annalen der Physik* **2**(1–2), 55–75 (1948).
2. T. Heyduk, "Measuring protein conformational changes by FRET/LRET," *Curr. Opin. Biotechnol.* **13**(4), 292–296 (2002).
3. E. Jares-Erijman and T. Jovin, "FRET imaging," *Nat. Biotechnol.* **21**(11), 1387–1395 (2003).
4. H. Wallrabe and A. Periasamy, "Imaging protein molecules using FRET and FLIM microscopy," *Curr. Opin. Biotechnol.* **16**(1), 19–27 (2005).
5. L. Loura, et al., "FRET analysis of domain formation and properties in complex membrane systems," *Biochim. Biophys. Acta—Biomembr.* **1788**(1, Sp. Iss. SI), 209–224 (2009).
6. J. Silvius and I. Nabi, "Fluorescence-quenching and resonance energy transfer studies of lipid microdomains in model and biological membranes," *Mol. Membr. Biol.* **23**(1), 5–16 (2006).
7. A. Kenworthy, "Peering inside lipid rafts and caveolae," *Trends Biochem. Sci.* **27**(9), 435–438 (2002).
8. H. Wallrabe, et al., "Confocal FRET microscopy to measure clustering of ligand-receptor complexes in endocytic membranes," *Biophys. J.* **85**(1), 559–571.
9. J. Farinha and J. Martinho, "Resonance energy transfer in polymer nanodomains," *J. Phys. Chem. C* **112**(29), 10591–10601 (2008).
10. J. Yang, et al., "Energy transfer study of symmetric polyisoprene-poly(methyl methacrylate) diblock copolymers bearing dyes at the junctions: dye orientation," *Macromolecules* **38**(4), 1256–1263 (2005).
11. R. Capeta, J. Poveda, and L. Loura, "Non-uniform membrane probe distribution in resonance energy transfer: application to protein-lipid selectivity," *J. Fluoresc.* **16**(2), 161–172 (2006).
12. M. Acasandrei, et al., "Two-dimensional Forster resonance energy transfer (2-DFRET) and the membrane raft hypothesis," *Chem. Phys. Lett.* **419**(4–6), 469–473 (2006).
13. K. Towles, et al., "Effect of membrane microheterogeneity and domain size on fluorescence resonance energy transfer," *Biophys. J.* **93**(2), 655–667 (2007).
14. G. Gorbenko, et al., "Resonance energy transfer study of lysozyme-lipid interactions," *Biochim. Biophys. Acta-Biomembr.* **1778**(5), 1213–1221 (2008).
15. M. Anikovsky, et al., "Resonance energy transfer in cells: a new look at fixation effect and receptor aggregation on cell membrane," *Biophys. J.* **95**(3), 1349–1359 (2008).
16. L. Pisterzi, et al., "Oligomeric size of the M-2 muscarinic receptor in live cells as determined by quantitative fluorescence resonance energy transfer," *J. Biol. Chem.* **285**(22), 16723–16738 (2010).
17. V. Raicu, et al., "Protein interaction quantified in vivo by spectrally resolved fluorescence resonance energy transfer," *Biochem. J.* **385**(1), 265–277 (2005).
18. E. Yeow and A. Clayton, "Enumeration of oligomerization states of membrane proteins in living cells by homo-FRET spectroscopy and microscopy: theory and application," *Biophys. J.* **92**(9), 3098–3104 (2007).
19. M. Li, et al., "A fluorescence energy transfer method for analyzing protein oligomeric structure: application to phospholamban," *Biophys. J.* **76**(5), 2587–2599 (1999).
20. P. Wolber and B. Hundson, "Analytical solution to the Forster energy transfer problem in 2 dimensions," *Biophys. J.* **28**(2), 197–210 (1979).
21. D. Singh and V. Raicu, "Comparison between whole distribution- and average-based approaches to the determination of fluorescence resonance energy transfer efficiency in ensembles of proteins in living cells," *Biophys. J.* **98**(10), 2127–2135 (2010).
22. C. Berney and G. Danuser, "FRET or no FRET: a quantitative comparison," *Biophys. J.* **84**(6), 3992–4010 (2003).
23. P. Frederix, et al., "Dynamic Monte Carlo simulations to model FRET and photobleaching in systems with multiple donor-acceptor interactions," *J. Phys. Chem. B* **106**(26), 6793–6801 (2002).
24. M. Frazier, et al., "Investigation of domain formation in sphingomyelin/cholesterol/POPC mixtures by fluorescence resonance energy transfer and Monte Carlo simulations," *Biophys. J.* **92**(7), 2422–2433 (2007).
25. D. Zimet, et al., "Calculation of resonance energy transfer in crowded biological membranes," *Biophys. J.* **68**(4), 1592–1603 (1995).
26. B. Snyder and E. Freire, "Fluorescence energy transfer in 2 dimensions – a numerical solution for random and non-random distributions," *Biophys. J.* **40**(2), 137–148 (1982).
27. M. Kiskowski and A. Kenworthy, "In silico characterization of resonance energy transfer for disk-shaped membrane domains," *Biophys. J.* **92**(9), 3040–3051 (2007).
28. B. Corry, D. Jayatilaka, and P. Rigby, "A flexible approach to the calculation of resonance energy transfer efficiency between multiple donors and acceptors in complex geometries," *Biophys. J.* **89**(6), 3822–3836 (2005).
29. S. Koushik, P. Blank, and S. Vogel, "Anomalous surplus energy transfer observed with multiple FRET acceptors," *PLoS ONE* **4**(11) (2009).
30. J. Lakowicz, *Principles of Fluorescence Spectroscopy.*
31. Z. Gryczynski, J. Lubkowski, and E. Bucci, Intrinsic fluorescence of hemoglobins and myoglobins," in *Fluorescence Spectroscopy," Volume 278 of Methods in Enzymology*, pp. 538–569 (1997).
32. B. Corry, et al., "Conformational changes involved in MscL channel gating measured using FRET spectroscopy," *Biophys. J.* **89**(6), L49–L51 (2005).
33. B. Corry, et al., "An improved open-channel structure of MscL determined from FRET confocal microscopy and simulation," *J. Gen. Physiol.* **136**(4), 483–494 (2010).
34. B. Adair and D. Engelman, "Glcyophorin-A helical transmembrane domains dimerize in phospholipids-bilayers a resonance energy transfer study," *Biochemistry* **33**(18), 5539–5544 (1994).
35. V. Raicu, "Efficiency of resonance energy transfer in homo-oligomeric complexes of proteins," *J. Biol. Phys.* **33**(2), 109–127 (2007).
36. R. Varma and S. Mayor, "GPI-anchored proteins are organized in submicron domains at the cell surface," *Nature* **394**(6695), 798–801 (1998).
37. A. Kenworthy and M. Edidin, "Distribution of a glycosylphosphatidylinositol-anchored protein at the apical surface of MDCK cells examined at a resolution of < 100 angstrom using imaging fluorescence resonance energy transfer," *J. Cell Biol.* **142**(1), 69–84 (1998).
38. P. Sharma, et al., "Nanoscale organization of multiple GPI-anchored proteins in living cell membranes," *Cell* **116**(4), 577–589 (2004).
39. A. Kenworthy, N. Petranova, and M. Edidin, "High-resolution FRET microscopy of cholera toxin B-subunit and GPI-anchored proteins in cell plasma membranes," *Mol. Biol. Cell* **11**(5), 1645–1655 (2000).
40. D. Zacharias, et al., "Partitioning of lipid-modified monomeric GFPs into membrane microdomains of live cells," *Science* **296**(5569), 913–916 (2002).
41. K. Börjesson, et al., "Nucleic base analog FRET pair facilitating detailed structural measurements in nucleic acid containing systems," *J. Am. Chem. Soc.* **131**, 4288–4293 (2009).